UDC 520.84-17 *Astrofiz. Issled. (Izv. SAO)*, 1993, **36**, 107-117

SOFTWARE FOR REDUCTION OF SPECTRAL DATA OBTAINED WITH PANORAMIC DETECTORS OF THE 6 M TELESCOPE

V. V. VLASYUK
Special Astrophysical Observatory of the Russian AS,
Nizhnij Arkhyz 357147, Russia

Received December 16, 1991

ABSTRACT. *A software for processing of spectral data obtained with the panoramic detectors of the 6 m telescope is described. A large amount of simultaneously registered spectra (with the multiobject fiber spectrograph, multipupil spectrograph) needs creation of maximum automatized system for data processing. The main peculiarities of present detectors which influence the quality of the obtained spectral information are described, and methods of their account are suggested. The software can be used with both computers of EC and PC/AT classes. The processing procedure is described.*

Предлагается пакет программного обеспечения для обработки спектральных данных, получаемых на панорамных приемниках, используемых в настоящее время на 6-м телескопе. Большое количество одновременно регистрируемых спектров (мультиобъектный волоконный спектрограф, мультизрачковый растровый спектрограф) делают необходимым создание максимально автоматизированных процедур. Описаны основные особенности существующих приемников, влияющие на качество получаемой спектральной информации, и предложены методы для их учета в процессе обработки. Разработанное обеспечение может быть использовано как на ЭВМ класса ЕС ЭВМ, так и на ПЭВМ класса PC AT. Этапы обработки показаны на реальных наблюдательных данных.

I. INTRODUCTION

Introduction into practice of astrophysical observations on the 6 m telescope of a low-dispersion multiobject fiber spectrograph for investigation of faint objects, and then a multipupil mode of moderate resolution fiber spectrograph for studying extended objects has called for development of specific software which would allow for both the fact that the number of independent registered spectra amounts to 70-80 and the peculiarities of light detectors used for accumulation of data. For reduction of a large number of spectra we need to use the computer EC-1035 and to make the process as automatic as possible.

The appearance of personal computers in the past years has made it possible to create on the basis of the developed software convenient for a user and more efficient system which reduces considerably the time for processing and allows to obtain results directly in the course of observations.

2. PECULIARITIES OF THE DETECTOR

Design and principal characteristics of the fiber spectrograph have been described earlier (Afanasiev et al., 1992). We remind the peculiarities of the detector system which determine the reduction algorithms and general quality of astrophysical data obtained. Registration of spectra is performed with the TV panoramic detector and the system "Kvant" developed at the Leningrad Institute of Television (Afanasiev et al., 1986). The detector is a square matrix with a side size of 512 elements 30 μm each. The number of spectra detected at the same time is defined by the detector size and angular enlargement of the spectrograph. Depending on the optical layout the number of spectra may vary from 40 to 100. The spectrograph quality is not so good that at rather dense "packing" of spectra on a detector matrix partial overlapping of neighbouring wings becomes possible. This reduces contrast of spectral details, and for relatively bright of them leads to appearance of artifacts in the neighbouring spectra.

The sensitivity inhomogeneities caused by the detector design are comparatively large (up to 10 %). The distortions characteristic of all the systems employing image tubes reach 5-7 elements at the field margin. The spectral sensitivity of the detector determines the optimal spectral range for observations: from 4500 A to 7500 A. To reduce detector noise nitrogen vapour cooling is applied. Nevertheless, it is the main factor affecting the signal-to-noise in the integrated image, especially in the multipupil mode of observations, where the number of photocounts from the object is comparable with that of noise counts.

With the account of all above stated the entire procedure of reduction of obtained observational data may be divided into the following stages:

1) allowance for the detector local inhomogeneities;
2) correction of geometric distortions of spectra and their integration;
3) reduction of spectra to a uniform wavelength scale;
4) correction of spectra for the inhomogeneity of fiber transmission;
5) subtraction of the night-sky spectrum (for multiobject spectroscopy);
6) correction of spectral sensitivity, obtaining of true energy distribution in the spectra.

3. CORRECTION OF THE DETECTOR SENSITIVITY INHOMOGENEITIES

One of the reasons preventing from precise correction of observational data for the sensitivity inhomogeneity of the detector is the instability of the whole detecting system during the observations, which is due to both the instabilities of the detector and variable effect of the terrestrial magnetic field. Attempts to correct the inhomogeneities by way of ordinary division of the image spectra by flatfield integration leads to differentiation of the spatial structure of these inhomogeneities, which, of course, worsens the data quality.

For reliable correction of the detector inhomogeneities we have elaborated methods of data analysis based on the well known cross-correlation method for matching of objects. This method is described by Pratt (1982).

As a reference image, flatfield integration g(x,y) was used. To define accurately the form of nonlinear distortion of the detector surface in field of spectral data, f(x,y) both matrices f(x,y) and g(x,y), where x, y = 1...512 were divided into fragments of 64x64 elements. Then the location of the cross-correlation function (CCF) maximum was determined for each pair.

$$R_{fg}(x',y') = \sum_{xy}\sum f'(x,y)\cdot g'(x-x',y-y'),$$

where $f'(x,y)$ and $g'(x,y)$ have been obtained from the initial images and have a zero mean and a dispersion which equals 1. Owing to normalization the values of R_{fg} are within the limits [-1,1] and reach maximum at full coincidence of the fragments analyzed. The value of the CCF at maximum allows to judge on the degree of similarity of the fragments, i.e. how the structure peculiarities of the detector, presenting in the flatfield integration, manifest themselves in the obtained spectra. The coordinates of the maximum yield the value of the shift of the examined fragment relative to the reference in both coordinates.

An example of spectral image obtained with the multiobject fiber spectrograph and photon counting system is shown in Fig.1. As can be seen from the figure, the location of the spectra in the integrated image distorts essentially the spatial structure of inhomogeneities. Therefore for stable operation of the algorithm the data undergo high-frequency filtering by a linear recursive filter. The window size of the

filter has been chosen by us on the basis of characteristic size of spectral details and equals in most cases 5 elements. The result of image smoothing with such a filter was subtracted from the initial image, which resulted in the desired effect. Fig.2a displays a fragment of the two-dimensional CCF obtained without filtering the images being compared, and Fig.2b presents the same fragment after the high-frequency filtering. The effect of a noticeable improvement of the signal-to-noise ratio for the cross-correlation peak under consideration is evident. Typical CCF maximum values for spectral data are 0.10-0.30. The application of this technique to two images of uniform light flux yields values within 0.40-0.80.

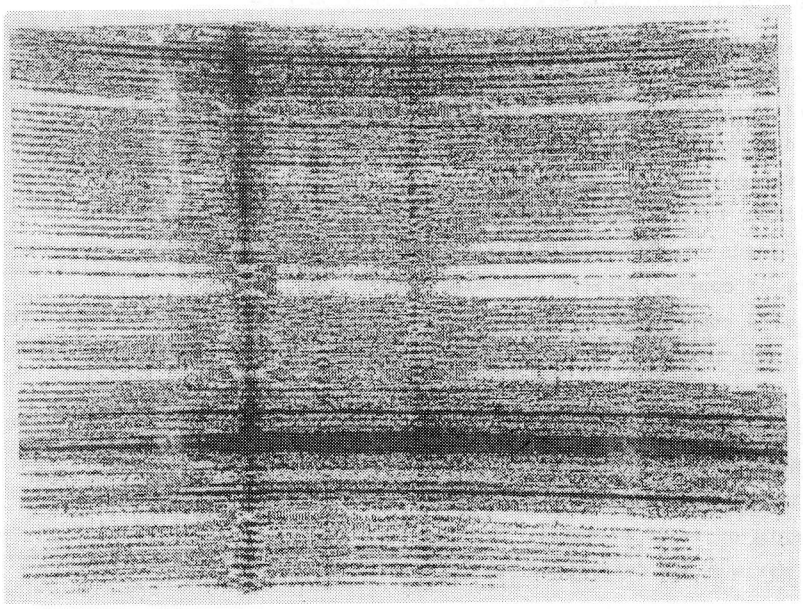

Fig.1. *The spectral image obtained with the multiobject fiber spectrograph of the 6 m telescope. The dispersion direction is from left to right. The spectral range is 4600-7700 ÅÅ. The bright details are the night-sky lines (from left to right are 5577 Å, 5890 Å, 6300 Å, and 6364 Å).*

The field of differential shifts in both coordinates thus obtained from all fragments of the image is approximated by a set of two-dimensional polynomials:

$$x' = a_0 \cdot x^2 + a_1 \cdot x \cdot y + a_2 \cdot y^2 + a_3 \cdot x + a_4 \cdot y + a_5,$$

$$y' = b_0 \cdot x^2 + b_1 \cdot x \cdot y + b_2 \cdot y^2 + b_3 \cdot x + b_4 \cdot y + b_5,$$

where x = 32, 96, 160,... 480, y = 32, 96,... 480 are the coordinates of the centers of the fragments, x', y' are the measured positions of the CCF peaks for each fragment. Constants a_i, b_i, i = 0...5 were defined by the least-squares method, the

weights of points (x_i, y_i) being determined with the account of the CCF peak value. The crosses in Fig.3 indicate the measured positions of the CCF peaks, their relative shift being magnified to be demonstrative, and the points of intercept of the curves on the same scale show the approximated position of each of the peaks.

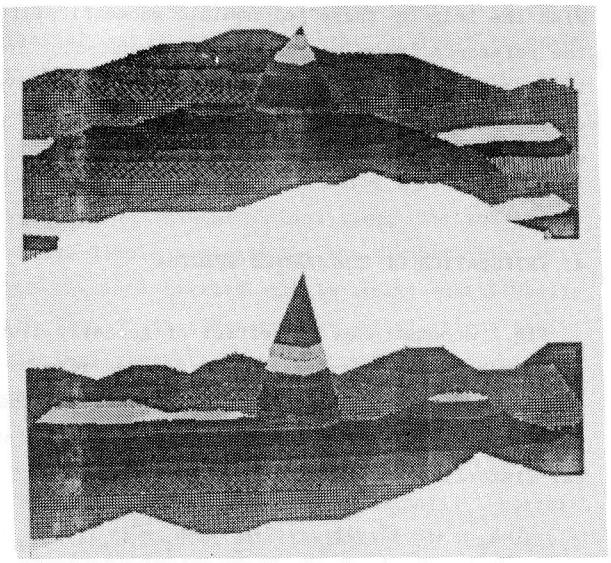

Fig.2. *Axonometrical representation of the central part of the cross-correlation function of fragments of spectral integration and flatfield: without spatial high-frequency filtering (top), after filtering removing the low-frequency component (bottom).*

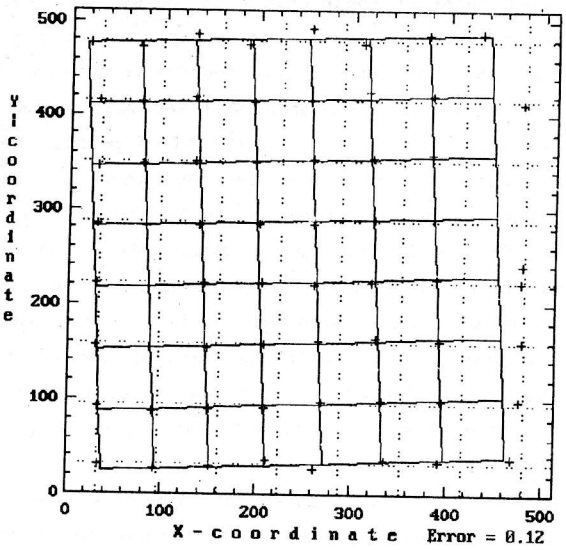

Fig.3. *The field of relative displacements of fragments of two images. The crosses mark the measured position of displacements, the lines connect their approximated positions.*

The smoothness of the picture and small deviations of the shifts in each of the fragments from the approximating polynomials guarantee accurate fit of the inhomoge-

neities in the integrations of spectra and flatfield. If for some reasons the contrast of the detector inhomogeneities in the image under investigation is very low, it will lead to the values of R_{fg} less than 0.1 and to a random scatter of the coordinates of its peaks over the field of the detector. The mean error of creation of polynomials for observational data does not, as a rule, exceed 0.15-0.2 of an element. With the help of these polynomials geometrical transformations of the data matrix to the reference image is performed. The detector instabilities mentioned above lead to the necessity of flatfield integration during several exposures of 1.5-2 hours. These exposures undergo the procedure described, then they are summed, and the total exposure is used as the reference image in the analysis of spectral data.

4. INTEGRATION OF THE CURVED SPECTRA

Fig. 1 demonstrates the effect of geometry distortion, which is characteristic of all systems with an image tube as the detector. This effect leads to curving of spectra and linear dispersion variation along the spectrum. For integration of individual spectra along the curved trajectories we are constructing a model of geometrical distortions of the system of the kind

$$y' = b_0 \cdot x^3 + b_1 \cdot x^2 \cdot y + b_2 \cdot x \cdot y^2 + b_3 \cdot y^3 + b_4 \cdot x^2 + b_5 \cdot x \cdot y + b_6 \cdot y^2 + b_7 \cdot x + b_8 \cdot y + b_9,$$

where x, y are the measured coordinates of fixed points, and y' are the corrected coordinates of these points in the system with the rectangular geometry. As the fixed points we use lines of the comparison spectrum registered between the exposures under the same conditions as the spectra we explore. For confident construction of the distortion model the number of fixed points must be about 40-50 and they must make a rectangular matrix of 6x6-8x8 fixed points. Here the fixed points in one line must naturally refer to one spectrum. The approximate positions (to an accuracy of 1-2 elements) of the fixed points is specified by a user. The coefficients b_i, i=0...9 are derived by the least-squares method. The mean error of the distortion model construction from the real data does not exceed, as a rule, 0.2-0.3 of an element. The error has random character and is caused by the determination accuracy of position of the fixed points. With the help of the coefficient b_i for each spectrum a curved aperture is formed in which the signal is summed. The aperture height depends on the distance between the neighbouring spectra and is usually assumed to be 3 or 5 elements of the detector.

When personal computers of IBM PC AT/386 type are used for data reduction, it seems possible to simplify the procedure of determining the parameters of geometric distortions. For this we would recommend to use the integrations of spectra of a continuous radiation source. Here we perform automatic identification of spectra on the basis of the assumption that they are all spatially separated.

Such procedure of integration is done with the spectra of the objects under study, the comparison spectrum and the spectrum of the continuous radiation source, and, when it is needed, with the night-sky spectra as well, which can be registered separately. As a comparison spectrum source we use in multiobject mode a vacuum lamp filled with a mixture of neutral gases He, Ne and Ar, and in the multipupil spectrograph (MPFS) a Xe+Ne+Ar one is used. The continuous radiation source was a filament lamp or the sky soon after sunset or not long before rise.

5. REDUCTION OF INDIVIDUAL SPECTRA

Because of a large amount of information contained in one image, we try to avoid as much as possible the user to take part in the procedures of reduction of individual spectra.

In the reduction of spectra to a uniform wavelength scale (linearization) the user needs only mark the position of lines in the comparison spectrum and the wavelengths corresponding to them for one of the spectra. Line identification for the comparison spectrum is described in the manual for observations with the scanner of the 6 m telescope and with the long-slit spectrograph UAGS (Lipovetsky et al., 1990; Burenkov et al., 1987). Usually spectrum integration over the field of the detector is executed consecutively as the coordinate along which the spectra are aligned increases. Therefore the mask for the position of spectral lines introduced by the user is applied to each of the spectra, adjusting to variations of line position. The accuracy of determination of the line position, both single and many blends, is not more than 0.2 of an element. As the position of a spectral line we use its center of gravity obtained in a window occupying 5 elements around the line maximum. The dispersion curve is constructed as a 3rd-degree polynomial which approximates by the least-squares method the wavelength-coordinate dependence:

$$\lambda(x) = a_0+a_1\cdot x+a_2\cdot x^2+a_3\cdot x^3.$$

The first approximation for the polynomial is constructed using the weights which are determined by the accuracy of defining the line position. For stable determination of the parameters of the dispersion curve the procedure, well known from the theory of robust estimation (Hampel, 1989), is repeated: the root-mean-square deviation of points σ from the dependence $\lambda(x)$ is defined. The weights of the points having a deviation less than 2 σ remain unchanged, the weights of the points with a larger deviation are lowered, the weights of the points whose deviation exceeds 3 σ are set to zero, and further they are not used in the construction of the dispersion curve. Application of this technique to the spectra obtained with the multiobject fiber spectrograph (MFS) with a reciprocal dispersion of about 7 A/channel yields a mean linearization error of about 1.5 Å. It should be added that in linearization of

spectra which contain some known bright emission feature, for example, the lines [OI] λ 5577 or NaI λλ 5889-5896 Å it can also be used in the procedure.

As has been noted previously (Afanasiev et al., 1992) the fibers used to transfer the light to the spectrograph slit have different transmission. To correct for this effect we use the linearized spectra of the continuous radiation source. The function describing the transmission of the i-th fiber is defined by us as

$$f_i(\lambda) = a_i + b_i \cdot \lambda,$$

where a_i, b_i are derived by the least-squares method from the result of division of the i-th spectrum by the spectrum adopted as standard and preliminarily smoothed. The estimates show the accuracy of correction of transmission inhomogeneity to be within 5-7 %.

After such reduction the subsequent stages of processing become possible:

1) subtraction of an averaged night-sky spectrum, if several such spectra were registered simultaneously during the observation;
2) determination of energy distribution in the spectra, if it was possible to obtain a spectrum with a known distribution;
3) construction of maps of spatial distribution of radiation in the selected spectral intervals;
4) determination of astrophysical parameters from the spectra.

Stages 1,2 and 4 are usually fulfilled at the data reduction obtained with the multiobject spectrograph, stages 2, 3, 4 - in the processing of observational results obtained with the multipupil fiber spectrograph (Afanasiev et al., 1990 a).

6. EXAMPLES OF ASTROPHYSICAL DATA PROCESSING

The reduction procedures described here can be illustrated by the results of the 6 m telescope observations with the MFS of the selected sky areas with the aim of study evolution of active extragalactic objects. One of such areas is the field of SA57, which has been previously investigated on the 6 m telescope by the method of multi-slit spectroscopy (Afanasiev et al., 1990b, 1990c). The total exposure of the spectra of this field was about 2 hours. Due to the absence of a spectral standard the reduced spectra are not corrected for spectral sensitivity of the detector.

Fig.4a presents the linearized spectra of an emission galaxy before and after subtraction of the background spectrum, and also the night-sky spectrum used for subtraction. The integral B magnitude of this galaxy is 18.73. A number of absorption lines together with the emission H_α are confidently identified in the spectrum. From these lines we have defined the redshift of the galaxy to be equal to 0.125. Spectra of this galaxy taken with the multi-slit field spectrograph and TV scanner are shown in Fig.8 of the paper by Afanasiev et al. (1990b). They also show the presence of

emission lines, in particular, [OII] λ 3727.

Fig. 4b shows the spectra of one of the field stars before and after subtraction of the night-sky spectrum. As can be seen from the spectrum, this star is a dwarf of spectral class M0-M2. Its B magnitude is 19.45, and the B-V color index is 1.32, which is in good agreement with the mean color value for stars of this spectral class.

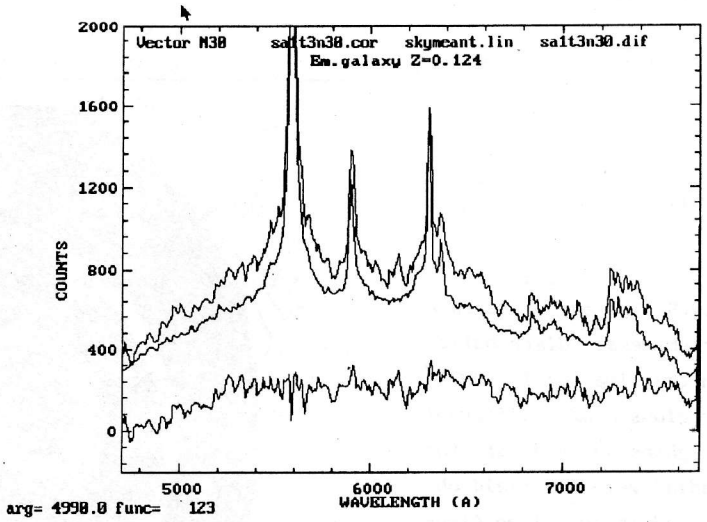

Fig. 4a. *The spectra of the objects obtained with the multiobject fiber spectrograph: the emission galaxy with z=0.125(a) and the star of spectral class M0-M2(b).*

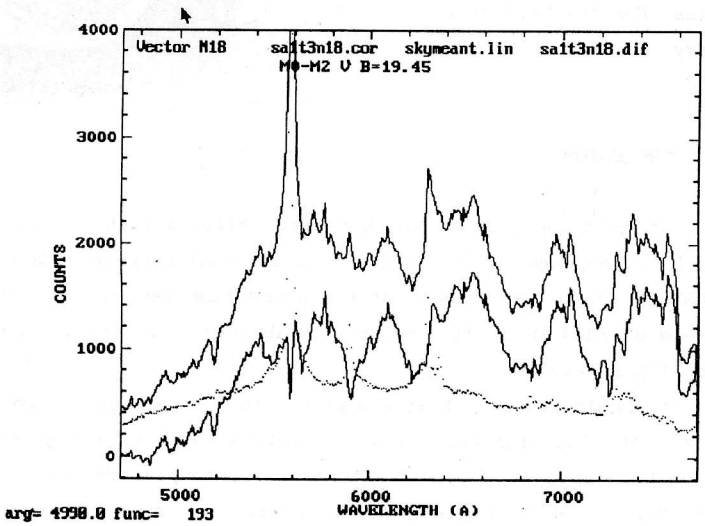

Fig. 4b.

Fig. 5 demonstrates the final reduction result of observations of the central part of one of the brightest Seyfert galaxy NGC 4151 with the multipupil fiber spectrog-

raph. The observations were made in the spectral range λλ 4400-5400 with a resolution of about 6 Å. This allowed to analyze the emission in the bright lines [OIII] 5007, 4959, H_β. The regions of different brightness demonstrate the surface brightness of emission in the line [OIII] λ 5007, and the isolines show the radial velocity field, obtained from the analysis of this line.

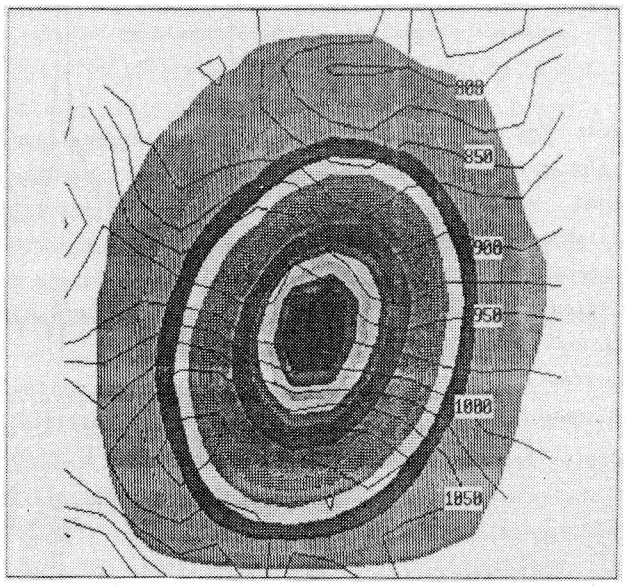

Fig.5. *The map of surface brightness distribution in the line [OIII] 5007 Å (regions of different brightness) and of the radial velocity field obtained in this line (isoline) for the Seyfert galaxy NGC 4151.*

7. CONCLUSION

The procedures described here are realized with a computer EC-1035 in the algorithmic language FORTRAN and with a personal computer IBM PC AT/386 in the languages FORTRAN and C. The amount of processor time needed for reduction of spectra of one field divided into 3-4 exposures is about 3 hours for EC-1035 and no more than 1 hour for IBM PC AT/386.

It should be noted that the work with the package of procedures has not been finished yet. The problems are to be solved: optimal integration of distorted spectra, reduction of data obtained with a charge-coupled device (CCD), analysis of profiles of complex spectral lines, and to create an integrated shell for the set of software programs, which makes the work of the user easier. It is natural that these problems will be solved using personal computers of IBM PC AT/386 class.

The author is indebted to V. L. Afanasiev and S. N. Dodonov for their help and fruitful discussions.

REFERENCES

Afanasiev V.L., Grudzinskij M.A., Kats B.M., Noshchenko V.S., Zukkerman I.I.: 1986, in: ASOIZ, **86**, Nauka, 182.

Afanasiev V.L., Vlasyuk V.V., Dodonov S.N., Sil'chenko O.K.: 1990a, *Preprint SAO,* **54**, Nizhnij Arkhyz.

Afanasiev V.L., Vlasyuk V.V., Dodonov S.N., Lorents Kh., Terebizh V.Yu.: 1990b, *Astrofiz. Issled. (Izv. SAO),* **32**, 31-65.

Afanasiev V.L., Vlasyuk V.V., Dodonov S.N., Lorents Kh. Terebizh V.Yu.: 1990c, *Astrofiz. Issled. (Izv. SAO),* **32**, 66-72.

Afanasiev V.L., Vlasyuk V.V., Dodonov S.N., Drabek S.V.: 1992, *Preprint SAO,* **83**, Nizhnij Arkhyz.

Burenkov A.N., Zhuravkov A.V., Shpekina N.K., Shtol' V.G.: 1987, *UAGS+KVANT: Description and instructions,* Nizhnij Arkhyz.

Lipovetsky V.A., Knyazev A.Yu., Shapovalova A.I.: 1990, *1024-channel scanner of BTA, Users' manual,* Nizhnij Arkhyz.

Prett U.: 1982, *Digital image processing,* **1,2**, M.: Mir.

Hampel F.R.: 1989, in: *Robustness in statistics,* M.: Mir.